

# Structure and evolution of the drainage system of a Himalayan debris-covered glacier, and its relationship with patterns of mass loss

Douglas I. Benn<sup>1</sup>, Sarah Thompson<sup>2</sup>, Jason Gulley<sup>3</sup>, Jordan Mertes<sup>4</sup>, Adrian Luckman<sup>2</sup> and Lindsey Nicholson<sup>5</sup>

<sup>1</sup> *School of Geography and Sustainable Development, University of St Andrews, UK*

<sup>2</sup> *Department of Geography, Swansea University, Swansea, UK*

<sup>3</sup> *School of Geosciences, University of South Florida, FL, USA*

<sup>4</sup> *Department of Geological and Mining Engineering and Sciences, Michigan Tech, MI, USA*

<sup>5</sup> *Institute for Atmospheric and Cryospheric Sciences, University of Innsbruck, Austria*

## Abstract

We provide the first synoptic view of the drainage system of a Himalayan debris-covered glacier and its evolution through time, based on speleological exploration and satellite image analysis of Ngozumpa Glacier, Nepal. The drainage system has several linked components: 1) a seasonal subglacial drainage system below the upper ablation zone; 2) supraglacial channels allowing efficient meltwater transport across parts of the upper ablation zone; 3) sub-marginal channels, allowing long-distance transport of meltwater; 4) perched ponds, which intermittently store meltwater prior to evacuation via the englacial drainage system; 5) englacial cut-and-closure conduits, which may undergo repeated cycles of abandonment and reactivation; 6) a 'base-level' lake system (Spillway Lake) dammed behind the terminal moraine. The distribution and relative importance of these elements has evolved through time, in response to sustained negative mass balance. The area occupied by perched ponds has expanded upglacier at the expense of supraglacial channels, and Spillway Lake has grown as more of the glacier surface ablates to base level. Subsurface processes play a governing role in creating, maintaining and shutting down exposures of ice at the glacier

surface, with a major impact on spatial patterns and rates of surface mass loss. Comparison of our results with observations on other glaciers indicate that englacial drainage systems play a key role in the response of debris-covered glaciers to sustained periods of negative mass balance.

## **1. Introduction**

Debris-covered glaciers in many parts of the Himalaya have undergone significant surface lowering in recent times (Kääb et al., 2012), with net losses of several tens of metres since the 1970s (Bolch et al., 2008a, 2011). Glacier thinning and reduced surface gradients have resulted in lower driving stresses and ice velocities, and large parts of many glaciers are now stagnant or nearly so (Bolch et al., 2008b; Quincey et al., 2009). These morphological and dynamic changes have encouraged formation of supraglacial ponds and lakes and increased water storage within glacial hydrological systems (Quincey et al., 2007; Benn et al., 2012). Where lakes form behind dams of moraine and ice, volumes of stored water can be as high as  $10^8 \text{ m}^3$ , in some cases posing considerable risk of glacier lake outburst floods (GLOFs) (Yamada, 1998; Richardson and Reynolds, 2000; Kattelman, 2003).

Several studies have shown that the development and enlargement of englacial conduits play an important role in the evolution of debris-covered glaciers during periods of negative mass balance (e.g. Clayton, 1964; Kirkbride, 1993; Krüger, 1994; Benn et al., 2001, 2009, 2012; Gulley and Benn, 2007; Thompson et al., 2016). The collapse of conduit roofs can expose areas of bare ice at the glacier surface, locally increasing ablation rates. Additionally, areas of subsidence associated with englacial conduits create closed hollows (dolines) that can evolve into supraglacial ponds, further increasing ice losses by calving. Conversely, supraglacial ponds can drain if a connection is made with the englacial drainage system, provided the pond is elevated above hydrological base level ('perched lakes' in the terminology of Benn et

al., 2001, 2012). Drainage of relatively warm water through the glacier leads to conduit enlargement, which in turn increases the likelihood of roof collapse, surface subsidence and ultimately new pond formation (Sakai et al., 2000; Miles et al., 2015). Because ablation rates around supraglacial pond margins are typically one or two orders of magnitude higher than those under continuous surface debris, ponds contribute disproportionately to overall rates of glacier ablation (Sakai et al., 1998, 2000, 2009; Thompson et al., 2016). By controlling the location and frequency of surface subsidence and pond drainage events, englacial conduits strongly influence overall ablation rates, and the volume of water that can be stored in and on the glacier (Benn et al., 2012).

Speleological investigations in debris-covered glaciers in the Khumbu Himal have demonstrated that englacial conduits can form by three processes: 1) 'cut-and-closure' or the incision of supraglacial stream beds followed by roof closure; 2) hydrologically assisted crevasse propagation, or hydrofracturing, which may route water to glacier beds; and 3) exploitation of secondary permeability in the ice (Gulley et al., 2009a, b; Benn et al., 2012). The relative importance of these processes in the development of glacial drainage systems, however, has not been investigated in detail. Furthermore, there are no data on the large-scale structure of englacial and subglacial glacial drainage systems in the Himalaya, or how they evolve during periods of negative mass balance. In this paper, we investigate the origin, configuration and evolution of the drainage system of Ngozumpa Glacier, using three complementary methods. First, speleological surveys of englacial conduits are used to provide a detailed understanding of their formation and evolution. Second, historical satellite imagery and high-resolution digital elevation models (DEMs) are used to identify past and present drainage pathways, glacier-wide patterns of surface water storage and release, and regions of subsidence. Finally, feature tracking on TerraSAR-X imagery is used to detect regions of the glacier subject to seasonal velocity fluctuations, as a proxy for variations in

subglacial water storage. Taken together, these methods provide the first synoptic view of the drainage system of a large Himalayan debris-covered glacier, and its influence on glacier response to recent warming.

## **2. Study area and methods**

Ngozumpa Glacier is located in the upper Dudh Kosi catchment, Khumbu Himal, Nepal (Fig. 1). It has three confluent branches: a western (W) branch flowing from the flanks of Cho Oyu (8188 m); a north-eastern (NE) branch originating below Gyachung Kang (7952 m); and an eastern (E) branch (Gaunara Glacier) nourished below a cirque of 6000 m peaks. The NE and E branches are no longer dynamically connected to the main trunk, which is fed solely by the W branch (Thompson et al., 2016). The equilibrium line altitude (ELA) is not well known. Google Earth images from 3 November 2009 (after the end of the ablation season) and 9 June 2010 (at the beginning of the monsoon accumulation season) show bare ice up to ~5700 m above sea level (a.s.l.) on all three branches, and this value is adopted as an approximate value of the ELA.

The lower ablation zone of the glacier is effectively stagnant, with little or no detectable motion on most of the E branch, or on the main trunk for ~6.5 km upglacier of the terminus (Bolch et al., 2008b; Quincey et al., 2009; Thompson et al., 2016). The lowermost 15 km of the glacier (below ~5250 m a.s.l.) is almost completely mantled with supraglacial debris. The debris cover thickens downglacier, reaching  $1.80 \pm 1.21$  m near the terminus (Nicholson, 2004; Nicholson and Benn, 2012). In common with other large debris-covered glaciers in the region, Ngozumpa Glacier has undergone significant surface lowering in recent decades, and the glacier surface now lies >100 m below the crestlines of the late Holocene lateral moraines (Bolch et al., 2008a, 2011).



The lower tongue of the glacier has a concave surface profile, with the overall gradient declining from 5.8° to 2.4° between 5,300 and 4,650 m (Fig. 2). The ice surface also becomes increasingly irregular downglacier, and below 5,000 m it forms numerous closed basins separated by mounds, ridges and plateaux with a relative relief of 50 - 60 m (Figs. 2 & 3). Most basins contain supraglacial ponds, which typically persist for a few years before draining (Benn et al., 2001; 2009, 2012; Gulley and Benn, 2007). Near the terminus of Ngozumpa Glacier, a system of lakes is ponded behind the terminal moraine (informally named Spillway Lake; Fig. 1). This lake system increased in area by around 10% per year from the early 1990s until 2009, but between 2009 and 2015 experienced a reduction of area and volume as a result of lake level lowering and redistribution of sediment (Thompson et al., 2012, 2016; Mertes et al., 2016). This hiatus is likely to be temporary and continued growth of the lake is expected in the coming years, as has been the case with other 'base-level lakes' in the region (Sakai et al., 2009).

We surveyed 2.3 km of englacial passages in Ngozumpa Glacier, using standard speleological techniques modified for glacier caves (Gulley and Benn, 2007). Conduit entrances were identified during systematic traverses of the glacier surfaces. Within each conduit, networks of survey lines were established by measuring the distance, azimuth and inclination between successive marked stations using a Leica Distomat laser rangefinder and a Brunton Sightmaster compass and inclinometer. Scaled drawings of passages in plan, profile and cross-section were then rendered *in situ*, and include observations of glaciostructural and stratigraphic features exposed in passage walls, thereby allowing the origin and evolution of conduits to be reconstructed in detail. In this paper, we focus on five conduits, which exemplify different stages of conduit formation, abandonment and reactivation. Three of the conduits have been previously described by Gulley and Benn (2007), but in this paper we revise our interpretation of their origin in some important

131 respects. Some of the conduits drained water from or fed water into supraglacial ponds, and  
132 in some cases it was possible to relate phases of conduit development to specific pond filling  
133 or drainage events, identified in satellite images.

134  
135 A range of optical imagery was used to map indicators of the large-scale structure of the  
136 drainage system (Table 1). The location of supraglacial channels and ephemeral supraglacial  
137 ponds were mapped using declassified Corona KH-4 imagery from 1965, Landsat 5 TM  
138 (2009), GeoEye-1 (9 June 2010 and 23 December 2012) and WorldView-3 (5 January 2015)  
139 imagery. The Corona and Landsat imagery was not co-registered or orthorectified beyond the  
140 standard terrain correction of the product, and was used to identify the presence / absence of  
141 larger ponds or channels and not to quantify rates of change.

142  
143 Geo-Eye-1 imagery from June 2010 and December 2012, and Worldview-3 imagery from  
144 January 2015 were acquired for a region covering 17.4 km<sup>2</sup> of the ablation area of the glacier.  
145 Three stereoscopic DEMs of 1 m resolution were constructed from the stereo multispectral  
146 imagery using the PCI Geomatica Software Package, and used to determine spatial patterns  
147 of elevation change. The construction and correction of the DEMs is discussed in detail in  
148 Thompson et al. (2016).

149  
150 The 2010 DEM was used to define the extent of individual surface drainage basins on the  
151 glacier surface. This was achieved by identifying surface elevation contours that entirely  
152 surround other contours of a lesser height. Each supraglacial catchment was then defined by  
153 the crestlines of ridges that separate the closed basins. Initially, we used 2 m contours but  
154 these produced a large number of very small 'basins', due to the high roughness of the  
155 bouldery glacier surface. Subsequently, we used 5 m contours that yielded a set of closed  
156 basins that closely matched the location of ephemeral supraglacial ponds on the glacier

surface. The extent of many basins changed between 2010 and 2015 due to ice-cliff backwasting, although all basins persisted through the period covered by the DEMs. It was not possible to delineate basins on the historical Corona or Landsat imagery because our methods depend on the availability of DEMs and cannot be applied to mono images.

Glacier surface velocities were derived using feature tracking between synthetic aperture radar images acquired by the TerraSAR-X satellite on 19 September 2014, 18 and 29 January 2015 and 5 January 2016. Feature tracking was done using the method of Luckman et al. (2007), which searches for a maximum correlation between evenly spaced subsets (patches) of each image giving the displacement of glacier surface features which are converted to speed using time delay between images. Image patches were  $\sim 400$  m x 400 m in size and sampled every 40 m producing a spatial resolution of between 40 and 400 m depending on feature density. Based on feature matching precise to one pixel (2 m), precision of the measured velocities is  $0.006$  m day<sup>-1</sup> over the annual (341 day) period and  $0.018$  m day<sup>-1</sup> over the winter (111 day) period. These values are used to define the threshold for detectable motion on the lower glacier.

### **3. Mechanisms of englacial conduit formation**

To provide an overview of processes of englacial conduit formation on the glacier, we describe two sites in detail (NG-04 and NG-05), then briefly describe and reinterpret three previously published sites (NG-01, NG-02 and NG-03; Gulley and Benn, 2007).

#### **3.1 NG-04**

*Description:* Conduit NG-04 (27°57'24"N, 86°41'55" E; 4805 m a.s.l.) was surveyed in November 2009, and consisted of a main passage (A) and two shorter side-passages (B and C) leading off to the west (Fig. 4). The main passage extended from a large hollow on the

glacier surface (Basin C-63 on Figs. 3e and 10a) for a distance of at least 473 m, where the survey was discontinued due to deep standing water on the cave floor. Side-passage B also connected with a basin on the glacier surface (Basin W-6, Figs. 3e and 10b). Side-passage C was at least 25 m long, but was not surveyed beyond this distance due to the evident instability of the highly fractured walls.

The main passage consisted of an upper level with a flat or gently inclined floor, and a lower narrow incised canyon. The passage was highly sinuous, with a sinuosity in the surveyed reach of 5.52. Near A4 (Fig. 4), there was a tight cutoff meander loop off the main passage (Fig. 5a). The base of the abandoned loop had a flat floor and lacked the incised lower level that was present elsewhere in the system. The upper floor level could also be traced along the walls of side passages B and C, which we interpret as twin remnants of a second meander cutoff. The floor of the upper level sloped gently downward from A1 to A14, rose from there to between A18 and A19, after which it descended once more. Sandy bedforms on the floor and scallops on the ice walls of this upper level indicate that water flow was from A1 towards A21.

Passage morphology in the upper level was very variable, including tubular, box-shaped, triangular and irregular sections (Figs. 4 & 5b-d). Throughout most of the system, planar structures were visible in the ceiling or walls of the upper level, running parallel to the passage axis with variable inclination. The structures took the form of: (1) 'sutures' at the line of contact between opposing walls (S: Fig. 4; Fig. 5b, c), (2) intermittent narrow voids (V: Fig. 4; Fig. 5c), and (3) bands of sorted sand or gravel a few cm thick (SB: Fig. 4; Fig. 5d). Some of the voids increased in width inward, in some cases opening out into gaps tens of cm across. In some places, bands of sorted sediment could be traced laterally into open voids or sutures. At several points along the main passage, a pair of planar structures occurred on

opposite walls of the passage. Side-passage B had a narrow, meandering seam of dirty ice running along its ceiling, and in Passage C the walls tapered upward to meet at a ceiling suture.

The floor of the incised lower level in both parts of the main passage sloped down towards side passages B and C (arrows, Fig. 4). A pair of incised channels was confluent at C1, whereas a single incised channel was present in passage B, where its lower (western) end was blocked by an accumulation of ice and debris.

*Interpretation:* The partially debris-filled structures in the walls and ceiling of the upper level are closely similar to many examples of canyon sutures we have observed in cut-and-closure conduits in the Himalaya and Svalbard, marking the planes of closure where former passage walls have been brought together by ice creep and/or blocked by ice and debris (cf. Gulley et al., 2009a, b). Cut-and-closure conduits are typically highly sinuous and have variable cross sectional morphologies, ranging from simple *plugged canyons* (incised channels with roofs of névé), to *sutured canyons* (partially or completely closed by ice creep), *horizontal slots* (formed by lateral channel migration followed by roof closure), and *tubular passages* (where passage re-enlargement has occurred under pipe-full (phreatic) conditions (Gulley et al., 2009b). The tubular morphology of the upper passage in NG-04, combined with the sutures, voids and sediment bands in the walls and ceiling indicates that the passage has been re-enlarged under pipe-full conditions following an episode of almost complete closure. For example, the sub-horizontal bands of sorted sand on both conduit walls between A15 and A18 (Fig. 5d) suggest complete suturing of a low, wide reach (horizontal slot) prior to formation of the surveyed passage.

The tubular and box-shaped cross-profiles and undulating long-profile of the upper passage are consistent with fluvial erosion under pipe-full or phreatic conditions (cf. Gulley et al., 2009b). This contrasts with the canyon-like form and consistent down-flow slope of channels incised under atmospheric (vadose) conditions, typical of simple cut-and-closure conduits. The dimensions of the upper passage (typically 2 m high and 3 m wide) are consistent with high discharges. We conclude that the upper passage formed when water draining from a supraglacial pond in Basin C-63 exploited the remnants of an abandoned cut-and-closure conduit (Fig. 3e).

Following formation of the upper passage, the lower level was incised under vadose (non pipe-full) conditions when the system accessed a new local base level via side-passages B and C. We infer that this occurred when a cutoff meander loop between B1 and C2 was exposed by ice-cliff retreat in Basin W-6. Water flow between A1 and B2 continued in the same direction as before, but between A14 and A21 flow was reversed and discharge much reduced.

Evolution of conduit NG-04 can be summarized as follows: 1) a cut-and-closure conduit was formed by incision of a supraglacial stream; 2) this conduit was abandoned and almost completely closed, presumably after it lost all or most of its source of recharge following downwasting of the overlying glacier surface; 3) the conduit remnants were exploited and enlarged by water draining from a supraglacial pond in Basin C-63; and 4) surface ablation in Basin W-6 broke into the conduit, creating a new base level and initiating floor incision. This remarkable cave illustrates how relict drainage systems can be reactivated when connected to new sources of recharge, and demonstrates how patterns of drainage can change dramatically within a single system in response to changing surface topography.

### 3.2 NG-05

*Description:* In December 2009 a conduit portal was exposed in an ice cliff at the margin of Spillway Lake (27°56'36" N, 86°42'46" E, 4670 m a. s. l.; Figs. 3a and 6). This portal was one of the two main efflux points that discharged water into the lake from upglacier (Thompson et al., 2016). Access to the conduit could be gained via the frozen lake surface (Fig. 7a), although the lake ice was broken up each morning by debris falling from the melting glacier surface above, severely limiting the time available for survey. Consequently, only a short section could be mapped (Fig. 6). The conduit had two main levels, separated by a narrow, partially ice-filled canyon. The floor of the lower part was at lake level, and that of the upper level was 4.8 m higher, close to the summer monsoon level of the lake, as indicated by shorelines exposed around the lake margins. Several notches on the passage walls recorded intermediate water levels. The ice cliff above the upper level was obscured by a mass of icicles, but observations inside the cave showed that the roof tapered up into a narrow debris band or suture.

*Interpretation:* Although short, this passage is important for understanding the drainage system of Ngozumpa Glacier. The debris band and suture in the roof indicates that, like NG-04, the passage formed by a process of channel incision and roof closure. Additionally, the passage is graded to the seasonally fluctuating surface of Spillway Lake. We therefore conclude that the main drainage on the eastern side of the glacier consists of a cut-and-closure conduit graded to the hydrologic base level of the glacier. For several km upglacier of the portal, the debris-covered ice surface is highly irregular and broken into numerous closed basins, implying that the conduit evolved from a surface stream that predates significant downwasting of the glacier. The significance of these conclusions will be discussed later in the paper.

### 3.3 NG-01, 02 and 03

*Description:* NG-01, NG-02 and NG-03 (Fig. 3d) were mapped in December 2005, and described by Gulley and Benn (2007). NG-01 had carried water southward into a large basin on the glacier surface (Basin C-25, Fig. 10a), whereas NG-02 drained water southward out of the basin. NG-01 (27°57'58" N, 86°41'50" E) was a sinuous canyon passage with three main levels. Debris bands cropped out in the walls of the uppermost level throughout its length, either at the lateral margins of the passage or in the roof (Fig. 7b). The mid-level had a sub-horizontal floor, into which the canyon linking to the lower level had been incised (Fig. 7c). NG-02 (27°57'55" N, 86°41'51" E) was a sinuous canyon passage on two levels, extending in a southwesterly direction from the basin. The upper level had a circular cross profile, and an incised canyon beneath formed the lower level. A suture and debris band was exposed along the entire length of the ceiling of the upper passage, mirroring the planform of the passage (Fig. 7d). The lower level was an asymmetric flat-floored passage with a series of sills along the margins. NG-03 (27°57'52" N, 86°42'02" E) consisted of a single passage graded to a supraglacial pond in Basin E-19. Passage morphology varied between a low, wide semi-elliptical cross-section and a more complex form with an elliptical upper section separated by a narrow neck from a lower A-shaped section. At the top of the canyon, the ceiling narrowed to a narrow slot, terminating in a band of coarse, unfrozen sandy debris.

*Interpretation:* For much of their length, all three conduits follow the trend of debris bands in the walls or roof, leading Gulley and Benn (2007) to conclude that all were structurally controlled. The debris bands were originally interpreted as debris-filled crevasse traces that had been deformed during advection downglacier. When the original work was conducted, the cut-and-closure model had not been developed, and we had yet to learn how to recognize the diverse forms such conduits can take, especially in the later stages of their development. It is now apparent that these conduits have all the hallmarks of cut-and-closure conduits. The



continuity and sinuous planform of the debris bands is consistent with formation by the closure of incised canyons, rather than crevasse fills that had been deformed by ice flow. Crevasses in the upper part of the glacier ablation area tend to be short, discontinuous and oriented transverse to flow, unlike the observed debris bands in the conduit roofs, and ice deformation is unlikely to be capable of generating the highly sinuous patterns observed within the conduit debris bands.

We therefore reinterpret NG-01 – 03 as cut-and-closure conduits that have undergone cycles of incision, abandonment, partial closure and later reactivation in response to fluctuating patterns of recharge on the glacier surface. The circular and elliptical cross profiles observed in NG-02 and NG-03 are consistent with phases of phreatic passage enlargement, analogous to that in NG-04. Abandoned, incompletely closed conduits create hydraulically efficient flow paths, which can be readily exploited and enlarged when surface ablation brings them into contact with new sources of recharge.

#### **4. Drainage system structure**

In this section, we present evidence for the large-scale structure of the drainage system and patterns of water storage and release, using X-band radar and optical satellite imagery and high resolution DEMs from 2010, 2012 and 2015.

##### *4.1 Subglacial drainage system*

*Observations:* Direct observation of the subglacial drainage system was not possible. Instead, we use seasonal fluctuations in glacier surface velocity to infer areas subject to variable subglacial water storage. Mean daily ice velocities of the glacier between 29 January 2015 and 5 January 2016 are shown in Figure 8a. There is no detectable motion (i.e. greater than  $\sim 0.01 \text{ m day}^{-1}$ ) on the main trunk within  $\sim 6.5 \text{ km}$  of the terminus or on the lowermost  $6 \text{ km}$  of

the E branch. The W branch is the most active, with velocities of  $\sim 0.16 \text{ m day}^{-1}$  ( $\sim 60 \text{ m yr}^{-1}$ ) at 5300 m a.s.l., declining to near zero at 4900 m. The NE branch is slower, although velocities in its upper part could not be determined due to image 'lay-over' in steep terrain. The active part of the NE branch does not extend as far down as the confluence with the W branch, and a strip of stagnant ice  $\sim 100 - 200 \text{ m}$  wide extends  $\sim 3 \text{ km}$  down the eastern side of the main trunk from the confluence zone. Thus, neither the E nor the NE branch is dynamically connected to the main trunk.

Evidence for seasonal velocity fluctuations is shown in Fig. 8b, which shows mean daily velocities between 29 January 2015 and 5 January 2016 (341 days) minus mean daily velocities from 19 September 2014 to 18 January 2015 (111 days). Meteorological data from the Pyramid Weather Station, at 5050 m a.s.l. c. 12 km east of Ngozumpa Glacier (available through the Ev-K2-CNR SHARE program), indicate that air temperatures were consistently below freezing between the 25th of September 2014 and the 28th of May 2015, defining a minimum winter period for the upper ablation zone. The 111 day interval lies almost entirely within the winter period but is less than half of its total duration, so Figure 8b yields minimum values for a summer speed-up on the glacier. Most of the active parts of the glacier exhibit some speed-up, although it is much more pronounced in some areas than others. On the W branch, the greatest speed-up (by  $\sim 0.015 \text{ m day}^{-1}$  or  $\sim 10\%$ ) occurs above the confluence with the NE branch. Areas of lesser speed-up also occur on the main trunk below this point, although these are discontinuous and less than the margin of error so are likely to be artifacts. Only the northern side of the NE branch is affected by a seasonal speed-up. This area coincides with the tongue of clean ice that descends through the icefall below Gyachung Kang (Fig. 1). Patchy areas of apparent speed-up and slow-down occur elsewhere on the NE branch but may be artifacts. A small speed-up also affects the active part of the E branch, above 5350 m a.s.l.

364

365 *Interpretation:* The seasonal variations in ice velocities in the upper ablation zone are too  
366 large to be explained by changes in ice creep rates, which would require fluctuations in  
367 driving stress that are inconsistent with the observed surface elevation changes on the glacier  
368 (Thompson et al., 2016). We interpret the velocity data as evidence for variations in basal  
369 motion (sliding and/or subglacial till deformation) in response to changing subglacial water  
370 storage. This interpretation is supported by the spatial distribution of areas affected by the  
371 seasonal speed-up, which coincide with, or occur downglacier of, heavily crevassed ice.  
372 Much of the upper ablation area of Ngozumpa Glacier consists of icefalls with surface  
373 gradients up to 30°, and fields of transverse crevasses occur across the entire width of the W  
374 branch down to an elevation of 5270 m (a, Fig. 9). Below this zone, crevasses are largely  
375 absent, reflecting decreasing ice velocities and compressive flow (b, c, and d; cf. Fig. 8).  
376 Fields of transverse crevasses occur in the upper basin of the E branch, above ~5400 m.  
377 Crevasses allow meltwater to be routed rapidly to the bed, and the existence of multiple  
378 recharge points will encourage development of a distributed drainage system following the  
379 onset of the monsoon ablation season. The lack of a clear seasonal velocity response on the  
380 lowermost 10 km of the glacier suggests that subglacial water is transported along the main  
381 trunk in efficient conduits, possibly along the glacier margins (see Section 4.4).

382

#### 383 *4.2 Supraglacial channels*

384 *Observations:* Supraglacial stream networks are visible below the crevassed zones on all  
385 three branches of the glacier. The most extensive network occurs on the tongue of clean ice  
386 on the NE branch, where a set of sub-parallel channels descends from ~5180 m to the  
387 junction with the W branch at ~4990 m (Fig. 3b, c; Fig. 14a). There are several discontinuous  
388 supraglacial channels on the W branch between 5220 m and 5120 m a.s.l., including one  
389 along the eastern margin of the glacier. Supraglacial channels occur on both flanks of the E

branch below ~5100 m a.s.l. The channels converge at the junction with the main trunk, and after flowing over the glacier surface for several hundred metres the combined stream sinks in a large hollow in Basin E-11. Patterns of water storage and release in this hollow are discussed in Section 4.4.

*Interpretation:* Perennial supraglacial channels can only persist if the annual amount of channel incision exceeds the amount of surface lowering of the adjacent ice (Gulley et al., 2009b). The rate at which ice-floored channels incise is controlled by viscous heat dissipation associated with turbulent flow, and increases with discharge and surface slope (Fountain and Walder, 1998; Jarosch and Gudmundsson, 2012). Because supraglacial stream discharge is a function of surface melt rate and melt area, significant channel incision requires large catchment areas. Therefore, incised surface channels tend to occur only where potential catchments are not fragmented by crevasses or hummocky surface topography (Fig. 3). At present, these conditions are met in relatively limited areas of Ngozumpa Glacier, below crevassed areas and above hummocky debris-covered areas.

#### *4.3 Hummocky debris-covered areas and perched ponds*

*Observations:* Most of the lower ablation zone of the glacier (below ~5,000 m) consists of hummocky debris-covered topography, where the glacier surface is broken up into distinct closed depressions, each of which forms a separate surface drainage basin (Fig. 3d, e). Not including the Spillway Lake basin that drains externally, we defined 111 surface basins in this zone in 2010 (Fig. 10). Some surface basins also occur between 5,000 and 5,100 m on the W Branch, but these are typically small, shallow and ill-defined (Fig. 3). This part of the glacier is steeper ( $3.4^\circ$ ) and has lower relative relief (~10 m) than the lower glacier, and appears to be a transitional zone between the channelized upper ablation area and the hummocky debris-covered zone (Fig. 2). Surface basins along the east and west margins of

the glacier form a series of depressions within almost continuous lateral troughs, and are considered in Section 4.4. Here, we focus on the basins in the central part of the glacier (C1 - C69; Fig. 10a) and the terminal zone (T1 - 6, Fig. 10b).

Of the 70 basins in the central part of the glacier, 56 (80%) contained ponds in at least one of the three years covered by the Geo-Eye and Worldview imagery. Fifteen of the 42 ponds present in 2010 (36%) had disappeared by 2012 or 2015, whereas 14 basins that were empty in 2010 contained ponds in one or more of the later years. Almost all of the remainder underwent partial drainage and /or refilling. In contrast, the 5 ponds in the terminal zone of the glacier (below Spillway Lake) clearly exhibited stability. Four showed no significant change in area between 2010 and 2015, while the other showed an increase in area.

*Interpretation:* Observations on and below the glacier surface show that drainage of perched ponds occurs when part of the floor is brought into contact with permeable structures in the ice (Benn et al., 2001; Gulley and Benn, 2007). The characteristics of NG-01 - 05 (which all occur within the hummocky debris-covered zone) show that relict cut-and-closure conduits are the dominant cause of secondary permeability in the glacier, providing pre-existing lines of weakness along which perched ponds can drain.

The spatial extent and high temporal frequency of perched pond drainage events on the glacier (Fig. 10a) imply a high density of active or relict conduits within the ice. A rough estimate can be obtained by dividing the number of complete and partial drainage events (35) by the total area of basins in the central part of the glacier ( $4.62 \text{ km}^2$ ), yielding  $\sim 7.6$  relict conduit reaches per  $\text{km}^2$ . This is a minimum estimate, because additional conduit remnants could occur below and beyond the margins of observed ponds. Conversely, the number of pond filling events (23 over the 5 ablation seasons spanned by the imagery) shows that

drainage routes commonly become blocked. Conduit blockage processes have been described by Gulley et al. (2009b), and include accumulation of icicles or floor-ice at the end of the melt season and creep closure of opposing conduit walls. The interplay between drainage events and conduit blockage maintains a dynamic population of supraglacial ponds, which contribute significantly to ablation of the glacier, through absorption of solar radiation and ice melt, and calving (Thompson et al., 2016).

The stability of ponds in the terminal zone probably reflects a combination of factors. These ponds are flanked by stable slopes of thick debris, which inhibit pond growth by melt or calving. Furthermore, the ponds are located at or close to the hydrologic base level of the glacier, determined by the terminal moraine that encircles the glacier terminus, inhibiting drainage via relict conduits.

#### *4.4 Sub-marginal drainage*

*Observations:* Elevation differences between successive DEMs indicate linear zones of enhanced surface lowering along both margins of Ngozumpa Glacier, forming troughs along the base of the bounding lateral moraines (Thompson et al., 2016; Fig. 11). The inner moraine slopes consist of unvegetated, unconsolidated till, and undergo active erosion by a range of processes including rockfall, debris flow and rotational landslipping (Benn et al., 2012; Thompson et al., 2016). Although debris eroded from the moraine slopes is transferred downslope into the troughs, the troughs underwent surface lowering of 6 – 9 m from 2010 to 2015, with a total annual volume loss in the moraine-trough systems of  $\sim 0.4 \times 10^6 \text{ m}^3 \text{ yr}^{-1}$  (Thompson et al., 2016). This implies that a large volume of ice, debris or both is evacuated annually from below the lateral margins of the glacier.

The lateral troughs form a series of closed basins, 12 on the west side and 22 on the east (Fig. 10b). Eight of the basins in the west trough and 17 of those in the east contained a pond in 2010, 4 (W) and 7 (E) of which had completely drained by 2012 or 2015. Four new ponds appeared in the eastern trough in 2012 or 2015, and 1 (W) and 7 (E) underwent partial drainage and/or refilling. Three basins on the western side and one on the eastern side showed no fluctuations in pond area.

Benn et al. (2001) provided detailed descriptions of pond filling and drainage cycles in basins W-7 and W-5 (Lakes 7092 and 7093 in their terminology). In October 1998, basin W-7 contained three shallow ponds, but by October 1999 the basin was occupied by a single large pond and water level had risen by ~9 m. Pond area had increased from 17,890 m<sup>2</sup> to 52,550 m<sup>2</sup>, with 36% of the increase attributable to backwasting and calving of the surrounding ice cliffs. By September 2000, the pond had almost completely drained and only shallow ponds remained. Pond drainage occurred via an englacial conduit, which had been exposed by retreat of the pond margin. A pond in basin W-5 also underwent fluctuations in area and depth between 1998 and 2000, but did not completely drain during that time. Horodyskuj (2015) used time-lapse photography and a pressure transducer to document rapid pond-level fluctuations in basin W-5, including rises and falls of several metres within hours.

Short-term cycles of pond drainage and filling can also be demonstrated in other basins within the lateral trough systems using optical satellite imagery. Figure 12 shows a series of images of the east side of the glacier close to the junction with the E branch, where a supraglacial stream (Section 4.2) flows into a closed depression in Basin E-11 (Fig. 10b). A pond occupying the basin expanded in area between March and May 2009, but drained between June and August. In 2015 there is little evidence of the pond in January but a large pond is present in June.

493

494 *Interpretation:* Widespread, rapid subsidence along both margins of the glacier can be  
495 explained by enlargement and episodic collapse of sub-marginal conduits (Thompson et al.,  
496 2016). Potential internal ablation rates were calculated from energy losses associated with  
497 runoff and supraglacial pond drainage, and the resulting value of  $0.12$  to  $0.13 \times 10^6 \text{ m}^3 \text{ yr}^{-1}$  is  
498 around 30% of the measured volume losses in the moraine-trough systems on the stagnant  
499 part of the glacier, the difference being at least partly attributable to sediment evacuation by  
500 meltwater.

501

502 The sub-marginal conduits are perennial features of the glacier drainage system, and  
503 discharge water into Spillway Lake during the winter months. Winter discharge may partly  
504 reflect slow release of water from supraglacial and englacial storage, but it may also partly  
505 consist of subglacial water from the upper ablation zone (see Section 4.1). This hints at the  
506 possibility that the sub-marginal channels function as the downglacier continuations of the  
507 subglacial drainage system, in addition to carrying water transferred more directly from the  
508 glacier surface.

509

510 Much of the lower ablation zone appears to be bypassed by the sub-marginal conduits, as  
511 evidenced by widespread water storage in supraglacial ponds (Section 4.3). As noted above,  
512 water is intermittently discharged from ponds in the central part of the glacier into the lateral  
513 troughs via englacial conduits. Cycles of pond drainage and filling in lateral basins indicate  
514 intermittent connections between surface catchments and the sub-marginal meltwater  
515 channels (Fig. 10b). In some cases, drainage events can be directly attributed to exploitation  
516 of englacial conduits (Benn et al., 2001). The hourly changes in pond level recorded by  
517 Horodyskuj (2015) cannot be explained by conduit opening and blockage, and more likely  
518 reflect short-term fluctuations in recharge from surface melt and water release from storage.



#### 4.5 Spillway Lake

*Observations:* In 2010, the area of the Spillway Lake surface catchment was 0.8 km<sup>2</sup>, of which 0.27 km<sup>2</sup> was occupied by the lake system. All of the water leaving the glacier passes through Spillway Lake, entering via portals or upwellings at or close to lake level, and leaving via a gap in the western lateral moraine ~1 km from the glacier terminus (1: Fig. 13). (It is possible that water also exits the glacier via groundwater flow, although no springs have been observed in the frontal moraine ramp.) In 2009, conduit NG-05 (Fig. 6; Section 3.2) entered the NE corner of the Spillway Lake and is interpreted as the distal part of the eastern sub-marginal conduit. A second conduit portal visible at the NW lake margin in the same year is interpreted as the efflux point of the western sub-marginal stream. The evolution of the Spillway Lake system, and its implications for drainage system structure in this part of the glacier, are examined in Section 5.4 below.

#### 4.6 Summary

The evidence presented above demonstrates that the drainage system of Ngozumpa Glacier comprises six linked elements: 1) a seasonal subglacial drainage system below the upper ablation zone; 2) supraglacial channels allowing efficient meltwater transport across parts of the upper ablation zone; 3) sub-marginal channels, allowing long-distance transport of meltwater; 4) perched ponds, which intermittently store meltwater prior to evacuation via the englacial drainage system; 5) englacial cut-and-closure conduits, which may undergo repeated cycles of abandonment and reactivation; 6) a 'base-level' lake system (Spillway Lake) dammed behind the terminal moraine. These elements have a distinct spatial distribution (Fig. 14a). Evidence for seasonal subglacial water storage is restricted to active parts of the glacier downglacier of crevasse fields, where surface water can be routed to the bed. Supraglacial channels occur where surface catchments and discharge are large enough to

allow channel incision rates to outpace surface ablation rates. Thus, perennial channels only occur where the glacier surface is not broken up by crevasse fields or into small, closed basins. Perched ponds occur where the glacier surface is broken up into closed basins, where the overall gradient of the glacier is  $<2.4^\circ$ . The life cycle of perched ponds is governed by the location of englacial 'cut-and-closure' conduits and the frequency of connection and blockage events. Sub-marginal conduits occur below both flanks of the glacier, and transport water from supraglacial channels, intermittent drainage from perched ponds, and possibly the subglacial drainage system, into Spillway Lake. The lake lies at the hydrologic base level of the glacier, and its extent reflects the surface elevation of the glacier relative to the spillway through the terminal moraine.

## **5. Evolution of the drainage system**

In this Section, we present evidence for changes in drainage system structure through time, including features visible on Corona images from 1964 and 1965, speleological observations, and repeat surveys of Spillway Lake since 1999.

### *5.1 Supraglacial channels*

In 1964, a connected supraglacial drainage stream network was present on the eastern side of the main trunk above the junction with the E branch (10 - 8 km from the terminus, 4950 m to 4920 m a.s.l.) (Fig. 15a). By 2010, this part of the glacier had been broken up into basins E-7, E-8 and E-9, part of the lateral trough systems described in Section 4.4. Stream channels were no longer present, although a number of isolated elongate ponds occupied depressions close to some of the original channel locations (Fig. 15b). The depressions have an overall reduction in elevation to the south, but in detail they have up-and-down long profiles. In cross profile, they are U-shaped and become wider and deeper through time (Fig. 15c).

We hypothesize that the supraglacial channels became deeply incised and transitioned into cut-and-closure conduits, which continue to evacuate meltwater below the glacier margins despite fragmentation of the surface topography. Channel incision may have been encouraged by thickening debris cover (from melt-out of englacial debris) that would have reduced glacier surface lowering rates.

At the distal end of the eastern lateral trough, conduit NG-05 (Fig. 6) emerges into Spillway Lake. Passage morphology indicates that at this point the conduit formed by cut-and-closure (Section 3.2). Thus, there is evidence for a cut-and-closure origin of subsurface conduits at both ends of the eastern lateral trough. We therefore infer that the sub-marginal conduits originated as supraglacial streams that became incised below the surface. Such a scenario would require a continuous slope along both glacier margins. We conclude that supraglacial streams occurred along both margins before development of the current irregular topography, but transition to cut-and-closure conduits allowed these drainage routes to persist after break-up of the glacier surface.

## *5.2 Englacial conduits in the hummocky debris-covered zone*

Transition of drainages from supraglacial channels to cut-and-closure conduits appears to have been a widespread process on the glacier. The presence of sutures, planar voids and bands of sorted sediments in the ceilings and walls of conduits NG-01 - NG-05 record former episodes of channel incision. As was the case for the lateral channels, we infer that systems of supraglacial channels existed in the central part of the lower tongue before the glacier surface was broken up into small closed basins (Fig. 14c).

Differential surface ablation can eventually cause fragmentation and abandonment of cut-and-closure conduits, cutting off downstream reaches from former water sources. In

abandoned reaches, processes of passage closure dominate over those of enlargement, and systems gradually shut down. Because cut-and-closure conduits are generally located close to the glacier surface, shut-down is commonly incomplete. Zones of narrow voids or sutures with infills of unfrozen sediment may persist, forming meandering lines of high permeability through otherwise impermeable glacier ice.

Reactivation of abandoned conduits will occur if a new water source becomes available, and a conduit remnant connects this source with a region of lower hydraulic potential. These conditions are met on stagnant, low-gradient glacier surfaces. Supraglacial ponds in closed basins provide both reservoirs of water and regions of elevated hydraulic potential. Drainage is highly episodic, and water may be stored in supraglacial ponds for years before passing farther down the system.

On the debris-covered part of Ngozumpa Glacier, cut-and-closure is the dominant primary process of conduit formation and active and relict cut-and-closure conduits create a secondary permeability that can be exploited by water from supraglacial ponds. Debris-filled crevasse traces may provide additional lines of weakness in some cases, although this is likely a minor process. We have not observed hydrofracture-type conduits in the debris-covered area of Ngozumpa Glacier, although it is possible that they may form under compressive flow conditions as described on Khumbu Glacier by Benn et al. (2009). Hydrofracturing likely plays a dominant role in surface-to-bed drainage in the crevasse fields of the upper ablation zone.

### *5.3 Spillway Lake*

The recent history of Spillway Lake was discussed in detail by Thompson et al. (2012, 2016), and is briefly reviewed here. The present spillway through the SW side of the terminal

moraine has been in existence since at least 1965, when water emerged from the glacier and entered a small pond behind the lateral moraine (1: Fig. 13). In the following decades, the Spillway Lake system expanded upglacier from this point. On the Survey of Nepal map (Nepal Survey Department, 1997) based on aerial photographs taken in 1992, the lake has a ribbon-like form, extending NE for ~600 m from the spillway. The lake had essentially the same outline at the time of our first field survey in 1998, when water was observed to enter the lake via a subaerial portal and an upwelling point (Fig. 13; Benn et al., 2001; Thompson et al., 2012). Between 1998 and 1999, several chasms and holes opened up on the glacier surface north of the western portal, and by 2001 these had evolved into linear ponds and lakes (2: Fig. 13). Between 2001 and 2009, the Spillway Lake system underwent considerable expansion to the north, accompanied by upglacier migration of the portal locations (3, 4: Fig. 13).

The predominantly linear patterns of lake expansion, and the location of meltwater portals and upwellings, indicate that evolution of the Spillway Lake system was strongly preconditioned by the locations of shallow englacial conduits (a, b: Fig. 13). Conduit NG-05 (Section 3.4 and Fig. 6) and other examples exposed around the lake margins show that the drainage system consists of cut-and-closure conduits graded to lake level. This near-surface englacial conduit system provided pre-existing lines of weakness in the ice which, when opened up to the surface by internal ablation and collapse, were exploited by ice-cliff melting and calving processes.

Spillway Lake was thus established on a template provided by two englacial conduits (a & b, Fig. 13), which were confluent prior to 1992. As it expanded upglacier, Spillway Lake encroached on areas formerly occupied by perched ponds and incorporated former supraglacial basins. A recent example is Basin C-33, which forms an inlier within the

Spillway Lake catchment (Figs. 10a and 13). This basin contained a perched pond in 2009 and 2010, but this drained prior to December 2012 and has not reformed. It is likely that this basin will become entirely subsumed within the Spillway Lake catchment in the near future, as a consequence of ice-cliff backwasting.

#### *5.4 Changing drainage patterns on the glacier*

Comparison of the drainage system structure in 2010 with evidence on Corona imagery from 1964 shows an upglacier expansion of the area occupied by closed depressions and perched ponds, and the formation and upglacier expansion of the base-level Spillway Lake (Fig. 14b). The widespread occurrence of cut-and-closure conduits provides evidence of an even earlier stage in drainage evolution, when supraglacial channels extended along most of the glacier tongue and closed basins were absent or rare (Fig. 14c). The upglacier limit of supraglacial channels was similar in 1964 and 2010, due to the persistent location of crevasse fields in the upper ablation zone. The channels are likely to have had similar upglacier limits in earlier times, because of the strong topographic control of the crevasse fields. Figure 14c shows a hypothetical distribution of supraglacial channels on the glacier during the Little Ice Age and early 20th Century.

Ngozumpa Glacier has thus responded to a prolonged period of negative mass balance with a systematic reordering of its drainage system, characterized by less efficient evacuation of meltwater and greater amounts of storage. More recent elements of the drainage system retain a memory of older elements, and processes and patterns of ablation on the glacier continue to be influenced by active and relict channels and conduits. Former supraglacial channels preconditioned the location and density of cut-and-closure conduits, which in turn precondition the formation and drainage of perched ponds and provide templates for the expansion of Spillway Lake.

## **6. Comparison with other debris-covered glaciers**

Observations on other debris-covered glaciers in the Himalaya indicate that their drainage systems share many of the characteristics described in this paper. Seasonal velocity fluctuations have been documented on other large glaciers in the Mount Everest region and on Lirung glacier, Nepal (Benn et al., 2012; Kraaijenbrink et al., 2016), indicating surface-to-bed drainage and variations in subglacial water storage. Perennial supraglacial channels occur in the upper ablation zones of many glaciers, in places where catchments are not fragmented by crevasse fields or irregular surface topography (Gulley et al., 2009b; Benn et al., 2012). Continuity between a supraglacial channel and an englacial cut-and-closure conduit has been observed on Khumbu Glacier, clearly demonstrating the genetic relationship between the two features (Gulley et al. 2009b). Perched ponds are widespread on Himalayan debris-covered glaciers, and evidence for repeated filling and drainage (Watson et al., 2016; Miles et al., 2017) suggest that englacial conduits may play an important role in their life cycles. However, englacial conduits have only been explored in a few glaciers (Gulley and Benn, 2007; Gulley et al. 2009b; Benn et al. 2009), and much research remains to be done. Similarly, very little is known about possible sub-marginal channels in Himalayan glaciers, and our few attempts to enter these highly dynamic environments have been repulsed.

The upglacier expansion of the area occupied by closed depressions and perched ponds on Ngozumpa Glacier (Fig. 14) also appears to have occurred on other glaciers in the Everest region during the current period of negative mass balance. Iwata et al. (2000) noted an increase in the area occupied by high-relief hummocky topography on Khumbu Glacier from 1978 to 1995. The presence of cut-and-closure conduits below hummocky terrain on that glacier shows that these areas formerly supported supraglacial streams (Gulley et al., 2009b).

There is strong evidence on many glaciers that growth of base-level lakes is preconditioned by englacial conduits. For example, upglacier expansion of the proglacial lake at Tasman Glacier, New Zealand, has repeatedly followed the locations former chains of sink holes on the glacier surface (Kirkbride, 1993; Quincey and Glasser, 2009). Recently formed chains of ponds on the lower ablation zone of Khumbu Glacier, strongly suggests that the same process is underway on that glacier (Watson et al., 2016). The integrated picture of drainage system structure and evolution presented in this paper provides a framework for predicting what the future may have in store for other debris-covered glaciers in the region.

## **7. Summary and Conclusions**

This paper has provided the first synoptic interpretation of the drainage system of a Himalayan debris-covered glacier, including the spatial distribution of system components, their evolution through time, and their influence on processes and patterns of ablation. Our specific conclusions are as follows.

1) In the upper ablation zone, seasonal variations in ice velocity indicate routing of surface meltwater to the bed via crevasses, and fluctuations in subglacial water storage.

2) Systems of supraglacial channels occur where the glacier surface is uninterrupted by crevasses or closed depressions, allowing efficient evacuation of surface melt.

3) Active sub-marginal channels are evidenced by linear zones of subsidence along both margins of the glacier, and fluctuations in surface water storage and release. These channels likely formed from supraglacial channels by a process of cut-and-closure, and permit long-distance transport of meltwater through the ablation zone. Transport of sediment via the lateral channels destabilizes inner moraine flanks and delivers debris to the terminal zone, where it modulates ablation processes.

4) In the lower ablation zone (below ~5,000 m) the glacier surface consists of numerous closed drainage basins. Meltwater in this zone typically undergoes storage in perched ponds



before being evacuated via the englacial drainage system. Englacial conduits in this zone evolved from supraglacial channels by a process of cut-and-closure, and may undergo repeated cycles of abandonment and reactivation. Cut-and-closure is the dominant process of conduit formation on Ngozumpa Glacier, and is likely so on other debris-covered glaciers in the Himalaya.

5) Enlargement of englacial conduits removes ice mass that is not captured by surface observations until conduit collapse occurs, with the implication that observations of sudden surface lowering need not reflect sudden glacier mass loss over the same time period. Subsurface processes play a governing role in creating, maintaining and shutting down exposures of ice at the glacier surface, with a major impact on spatial patterns and rates of surface mass loss.

6) A large lake system (Spillway Lake) is dammed behind the terminal moraine, which forms the hydrologic base level for the glacier. Since the early 1990s, Spillway Lake has expanded upglacier, exploiting weaknesses formed by englacial conduits.

7) As part of the glacier response to the present ongoing period of negative mass balance, the structure of the drainage system has changed through time, characterized by decreasing efficiency and greater volumes of storage. Processes and patterns of ablation on the glacier are strongly influenced by active and relict elements of the drainage system. Former supraglacial channels evolved into cut-and-closure conduits, which in turn precondition the formation and drainage of perched ponds and provide templates for the expansion of Spillway Lake. Thus drainage elements that initially formed during earlier active phases of the glacier's history continue to influence its evolution during stagnation.

## **Acknowledgements**

Funding for ST was provided by the European Commission FP7-MC-IEF grant PIEF-GA-2012-330805, and for LN by the Austrian Science Fund (FWF) Elise Richter Grant (V309-

N26). Financial support for fieldwork in 2009 was provided by the University Centre in Svalbard and a Royal Geographical Society fieldwork grant to ST. Field assistance was given by Annelie Bergström and Alison Banwell. TerraSAR-X data were kindly provided by DLR under Project HYD0178. The meteorological data were collected within the Ev-K2-CNR SHARE Project, funded by contributions from the Italian National Research Council and the Italian Ministry of Foreign Affairs, and we thank Patrick Wagon of the IRD for collecting and releasing the 2014-2015 data used in this paper. Careful and constructive reviews by A. Sakai and D. Quincey are gratefully acknowledged.

## References

- Benn, D.I., Wiseman, S. and Warren, C.R. 2000. Rapid growth of a supraglacial lake, Ngozumpa Glacier, Khumbu Himal, Nepal. IAHS Publication 264 (*Symposium in Seattle 2000 – Debris Covered Glaciers*), 177-185.
- Benn, D.I., Wiseman, S. and Hands, K., 2001. Growth and drainage of supraglacial lakes on the debris-mantled Ngozumpa Glacier, Khumbu Himal. *Journal of Glaciology*, 47, 626-638.
- Benn, D.I., Kirkbride, M.P., Owen, L.A. and Brazier V. 2003. Glaciated valley landsystems. In: Evans, D.J.A. (ed.) *Glacial Landsystems*. Arnold, 372-406.
- Benn, D.I., Gulley, J., Luckman, A., Adamek, A. and Glowacki, P. 2009. Englacial drainage systems formed by hydrologically driven crevasse propagation. *Journal of Glaciology* 55 (191), 513-523.
- Benn, D.I., Bolch, T., Dennis, K., Gulley, J., Luckman, A., Nicholson, K.L., Quincey, D., Thompson, S. and Tuomi, R. and Wiseman, S. 2012. Response of debris-covered glaciers in the Mount Everest region to recent warming, and implications for outburst flood hazards. *Earth Science Reviews* 114, 156-174.
- Bolch, T., Buchroithner, M., Pieczonka, T. and Kunert, A. 2008a. Planimetric and volumetric glacier changes in the Khumbu Himal, Nepal, since 1962 using Corona, Landsat TM and ASTER data. *Journal of Glaciology* 54 (187), 592-600.
- Bolch, T., Buchroithner, M., Peters, J., Baessler, M. and Bajracharya, S. 2008b. Identification of glacier motion and potentially dangerous glacial lakes in the Everest region/Nepal using spaceborne imagery. *Natural Hazards and Earth System Science* 8, 1329-1340.
- Bolch, T., Pieczonka, T. and Benn, D.I. 2011 Multi-decadal mass loss of glaciers in the Everest area (Nepal Himalaya) derived from stereo imagery. *The Cryosphere* 5, 349-358.
- Clayton, L. 1964. Karst topography on stagnant glaciers. *Journal of Glaciology* 5: 107-112.

789 Fountain, A.G. and Walder J. 1998. Water flow through temperate glaciers. *Reviews of*  
790 *Geophysics* 36, 299-328.

791 Gulley, J. and Benn, D.I. 2007. Structural control of englacial drainage systems in Himalayan  
792 debris-covered glaciers. *Journal of Glaciology* 53, 399-412.

793 Gulley, J., Benn, D.I., Sreaton, L. and Martin, J. 2009a. Mechanisms of englacial conduit  
794 formation and implications for subglacial recharge. *Quaternary Science Reviews* 28  
795 (19-20), 1984-1999.

796 Gulley, J., Benn, D.I., Luckman, A. and Müller, D. 2009b. A cut-and-closure origin for  
797 englacial conduits on uncrevassed parts of polythermal glaciers. *Journal of Glaciology*  
798 55 (189), 66-80.

799 Hambrey M J, Quincey D J, Glasser N F, Reynolds J M, Richardson S J and Clemmens S  
800 2008 Sedimentological, geomorphological and dynamic context of debris-mantled  
801 glaciers, Mount Everest (Sagarmatha) region, Nepal. *Quaternary Science Reviews* 27  
802 2361–2389.

803 Hands, K.A. 2004. *Downwasting and supraglacial lake evolution on the debris-covered*  
804 *Ngozumpa Glacier, Khumbu Himal, Nepal*. Unpublished PhD thesis, University of St  
805 Andrews.

806 Hansen, O.H. 2001. Internal drainage of some subpolar glaciers on Svalbard. Unpublished  
807 MSc thesis, The University Centre in Svalbard.

808 Horodyskyj, U.N. 2015. Contributing factors to ice mass loss on Himalayan debris-covered  
809 glaciers. Unpublished Ph.D. thesis, University of Colorado at Boulder, 183 pages

810 Humlum O. Elberling B. Hormes A. Fjordheim K. Hansen OH. Heinemeier J. 2005. Late-  
811 Holocene glacier growth in Svalbard, documented by subglacial relict vegetation and  
812 living soil microbes. *The Holocene* 15: 396-407.

813 Iwata, S., Aoki, T., Kadota, T., Seko, K., Yamaguchi, S., 2000. Morphological evolution of  
814 the debris cover on Khumbu Glacier, Nepal, between 1978 and 1995. In: Nakawo, N.,

815 Fountain, A., Raymond, C. (eds.) Debris-covered glaciers. IAHS Publication 264, 3-  
816 11.

817 Jarosch, A.H. and Gudmundsson, M.T. 2012. A numerical model for meltwater channel  
818 evolution in glaciers. *The Cryosphere* 6, 493-503.

819 Kääb, A., Berthier, E., Nuth, C., Gardelle, J. and Arnaud, Y. 2012. Contrasting patterns of  
820 early twenty first century glacier mass change in the Himalayas. *Nature* 488, 495-498.s

821 Kirkbride, M.P. 1993. The temporal significance of transitions from melting to calving  
822 termini at glaciers in the central Southern Alps of New Zealand. *The Holocene* 3: 232-  
823 240.

824 Kraaijenbrink, P., Meijer, S.W., Shea, J.M., Pellicciotti, F., De Jong, S.M. and Immerzeel,  
825 W.W. 2016. Seasonal surface velocities of a Himalayan glacier derived by automated  
826 correlation of Unmanned Aerial Vehicle imagery.” *Annals of Glaciology* 57 (71): 103–  
827 13.

828 Krüger, J. 1994. Glacial processes, sediments, landforms, and stratigraphy in the terminus  
829 region of Myrdalsjökull, Iceland. *Folia Geographica Danica*, 21, 1-233.

830 Mertes, J., Thompson, S.S., Booth, A.D., Gulley, J.D. and Benn, D.I. 2016. A conceptual  
831 model of supraglacial lake formation on debris-covered glaciers based on GPR facies  
832 analysis. *Earth Surface Processes and Landforms* doi: 10.1002/esp.4068.

833 Miles, E. S., Pellicciotti, F., Willis, I. C., Steiner, J. F., Buri, P., & Arnold, N. S. 2015.  
834 Refined energy-balance modelling of a supraglacial pond, Langtang Khola, Nepal.  
835 *Annals of Glaciology* 57, 29-40.

836 Miles, E., Willis, I., Arnold, N., Steiner, J. and Pellicciotti, F. 2017. Spatial, seasonal and  
837 interannual variability of supraglacial ponds in the Langtang Valley of Nepal, 1999–  
838 2013. *Journal of Glaciology* 63 (237), 85-105.

839 Nakawo, M, Iwata, S., Watanabe, O. and Yoshida, M., 1986. Processes which distribute  
840 supraglacial debris on the Khumbu Glacier, Nepal Himalaya. *Annals of Glaciology* 8,  
841 129-131.

842 Survey of Nepal, 1996. 1:50,000 Topographical Map Sheet 2786 03: Namche Bajar. Survey  
843 Department, Ministry of Land Reform and Management, Kathmandu.

844 Nicholson, L.A. 2004. *Modelling melt beneath supraglacial debris: Implications for the*  
845 *climatic response of debris-covered glaciers*. PhD thesis, University of St Andrews,  
846 UK.

847 Nicholson, L.A. and Benn, D.I. 2006. Calculating ablation beneath a debris layer from  
848 meteorological data. *Journal of Glaciology* 52 (187), 463-470.

849 Nicholson, L. and Benn, D.I. 2012. Properties of natural supraglacial debris in relation to  
850 modelling sub-debris ice ablation. *Earth Surface Processes and Landforms* 38, 490-501.

851 Quincey, D.J. and Glasser, N.F. 2009. Morphological and ice-dynamical changes on the  
852 Tasman Glacier, New Zealand, 1990-2007. *Global and Planetary Change*, 68, 185-197.

853 Quincey, D.J., Richardson, S.D., Luckman, A., Lucas, R.M., Reynolds, J.M., Hambrey, M.J.  
854 and Glasser, N.F. 2007. Early recognition of glacial lake hazards in the Himalaya using  
855 remote sensing datasets. *Global and Planetary Change* 56, 137-152.

856 Quincey, D., Luckman, A. and Benn, D.I. 2009. Quantification of Everest-region glacier  
857 velocities between 1992 and 2002 using satellite radar interferometry and feature  
858 tracking. *Journal of Glaciology* 55 (192), 596-606.

859 Richardson, S.D. and Reynolds, J.M. 2000. An overview of glacial hazards in the Himalayas.  
860 *Quaternary International*, 65-66, 31-47.

861 Sakai, A., Nakawo, M. and Fujita, K. 1998. Melt rates of ice cliffs on the Lirung Glacier,  
862 Nepal Himalaya, 1996. *Bulletin of Glacier Research* 16, 57-66.

863 Sakai, A., Takeuchi, N., Fujita, K. and Nakawo, M. 2000. Role of supraglacial ponds in the  
864 ablation process of a debris covered glacier in the Nepal Himalayas. IAHS Publication  
865 264 (*Symposium in Seattle 2000 – Debris Covered Glaciers*), 119-130.

866 Sakai, A., Nishimura, K., Kadota, T. and Takeuchi, N. 2009. Onset of calving at supraglacial  
867 lakes on debris covered glaciers of the Nepal Himalaya. *Journal of Glaciology* 55, 909-  
868 917.

869 Thompson, S., Benn, D.I., Dennis, K. and Luckman, A. 2012. A rapidly growing moraine  
870 dammed glacial lake on Ngozumpa Glacier, Nepal. *Geomorphology* 145–146, 1-11.

871 Thompson, S., Benn, D.I., Mertes, J. and Luckman, A., 2016. Stagnation and mass loss on a  
872 Himalayan debris-covered glacier: processes, patterns and rates. *Journal of*  
873 *Glaciology* 62(233), 467-485.

874 Watanabe, O., Iwata, S. and Fushimi, H. 1986. Topographic characteristics in the ablation  
875 area of the Khumbu Glacier, Nepal Himalaya. *Annals of Glaciology* 8, 177-180.

876 Watson, C.S., Quincey, D.J., Carrivick, J.L. and Smith, M.W., 2016. The dynamics of  
877 supraglacial ponds in the Everest region, central Himalaya. *Global and Planetary*  
878 *Change* 142, 14-27.

879 Wessels, R.L., Kargel, J.S. and Kieffer, H.H. 2002. ASTER measurement of supraglacial  
880 lakes in the Mount Everest region of the Himalaya. *Annals of Glaciology* 34, 399-408.

881 Vuichard, D. and Zimmermann, M. 1987. The 1985 catastrophic drainage of a moraine-  
882 dammed lake, Khumbu Himal, Nepal: causes and consequences. *Mountain Research*  
883 *and Development* 7, 91-110.

884 Yamada, T., 1998. *Glacier lake and its outburst flood in the Nepal Himalaya*. Monograph  
885 No. 1, Data Centre for Glacier Research, Japanese Society of Snow and Ice, Japan, 96  
886 pp.

887

888

889 Table 1: Satellite imagery used in the paper

<b>Sensor</b>	<b>Product type</b>	<b>Resolution m</b>	<b>Acquisition date</b>	<b>Cloud cover (%)</b>
<b>Corona</b>	KH-4	3	04 Mar. 1965	-
<b>Landsat 5 TM</b>	Level T1	30	05 Mar. 2009	17
<b>Landsat 5 TM</b>	Level T1	30	08 May 2009	16
<b>Landsat 5 TM</b>	Level T1	30	09 Jun. 2009	28
<b>Landsat 5 TM</b>	Level T1	30	16 Aug. 2009	18
<b>GeoEye-1</b>	GeoStereo	PAN 0.46	09 Jun. 2010	3
	PAN/MSI	MSI 1.84		
<b>GeoEye-1</b>	GeoStereo	PAN 0.46	23 Dec. 2012	0
	PAN/MSI	MSI 1.84		
<b>WorldView-3</b>	GeoStereo	PAN 0.46	05 Jan. 2015	0
	PAN/MSI	MSI 1.84		

890

891

892



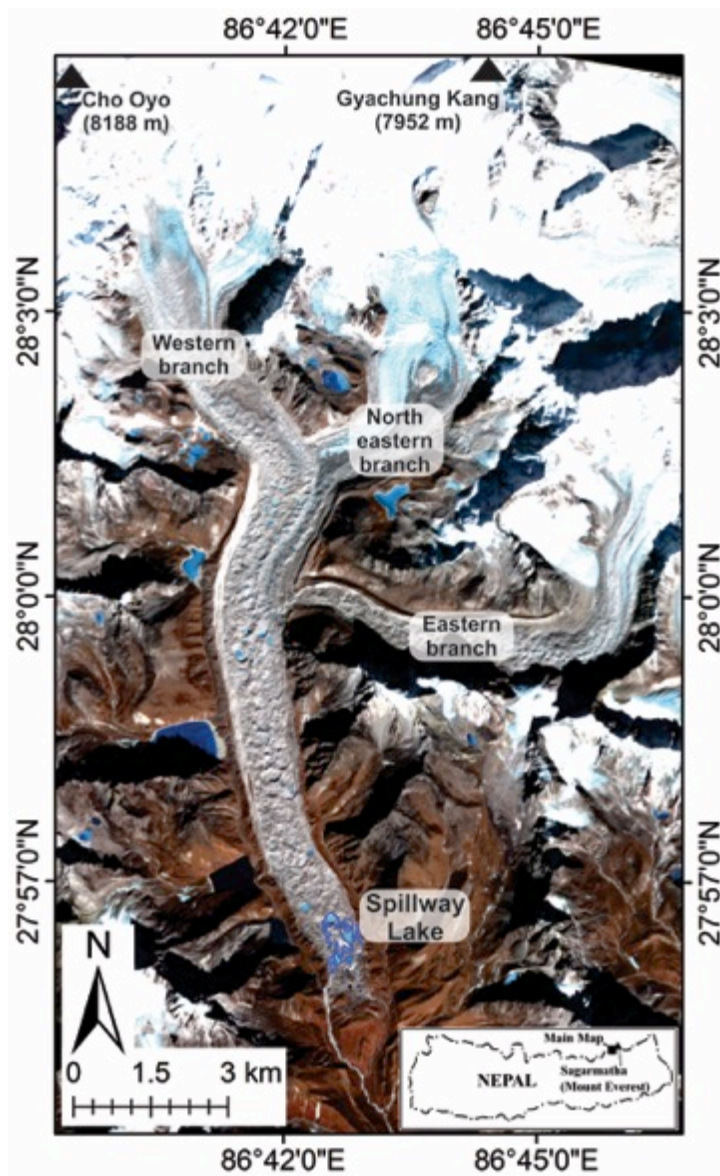


Fig. 1: Ngozumpa Glacier, showing the location of the three branches and Spillway Lake.  
Image: orthorectified GeoEye-1 from December 2012.

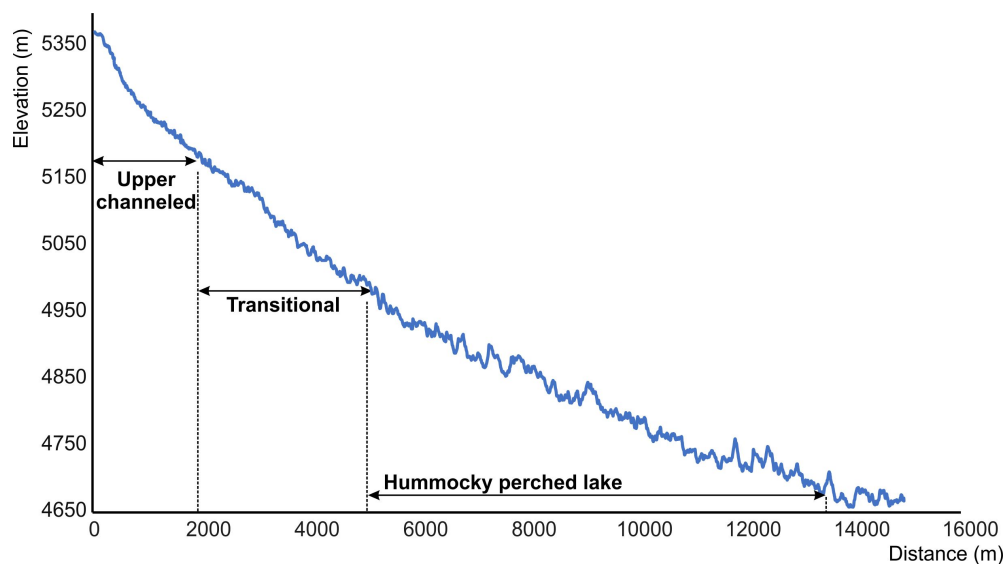


Figure 3: Longitudinal surface profile of the W branch and main trunk of Ngozumpa Glacier, showing downglacier changes in gradient and relative relief (see Fig. 2a for location). 'Upper channelled', 'Transitional' and 'Hummocky perched lake' refer to the drainage zones described in Sections 4.2 and 4.3.

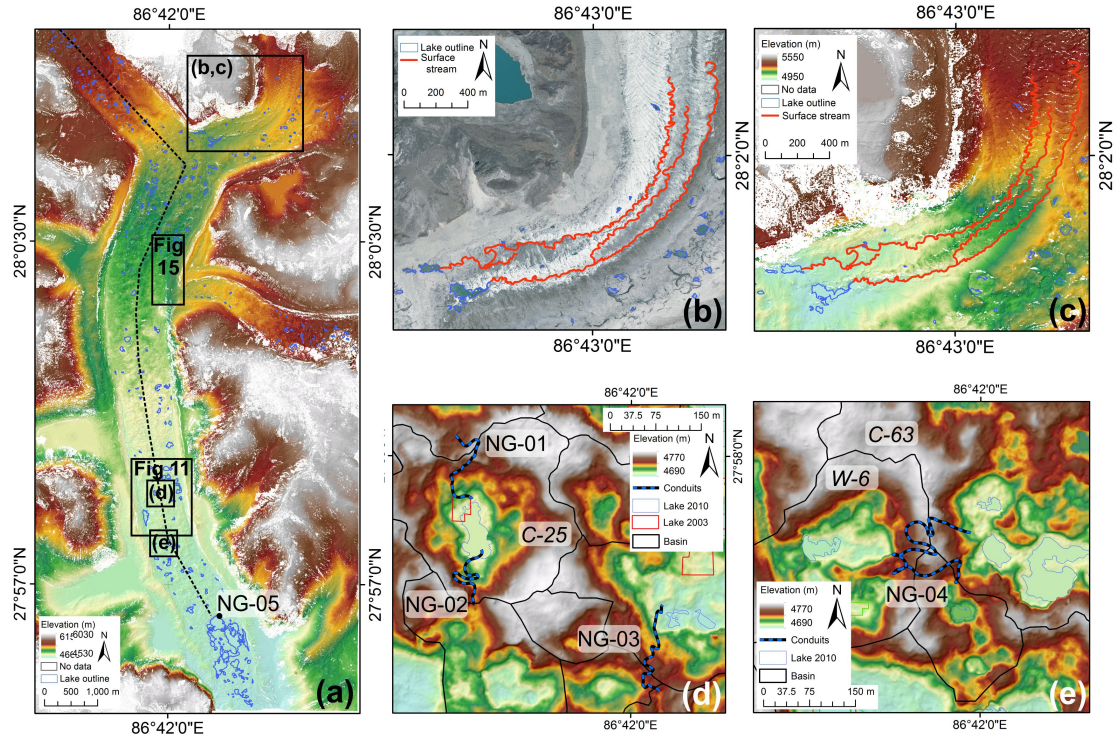
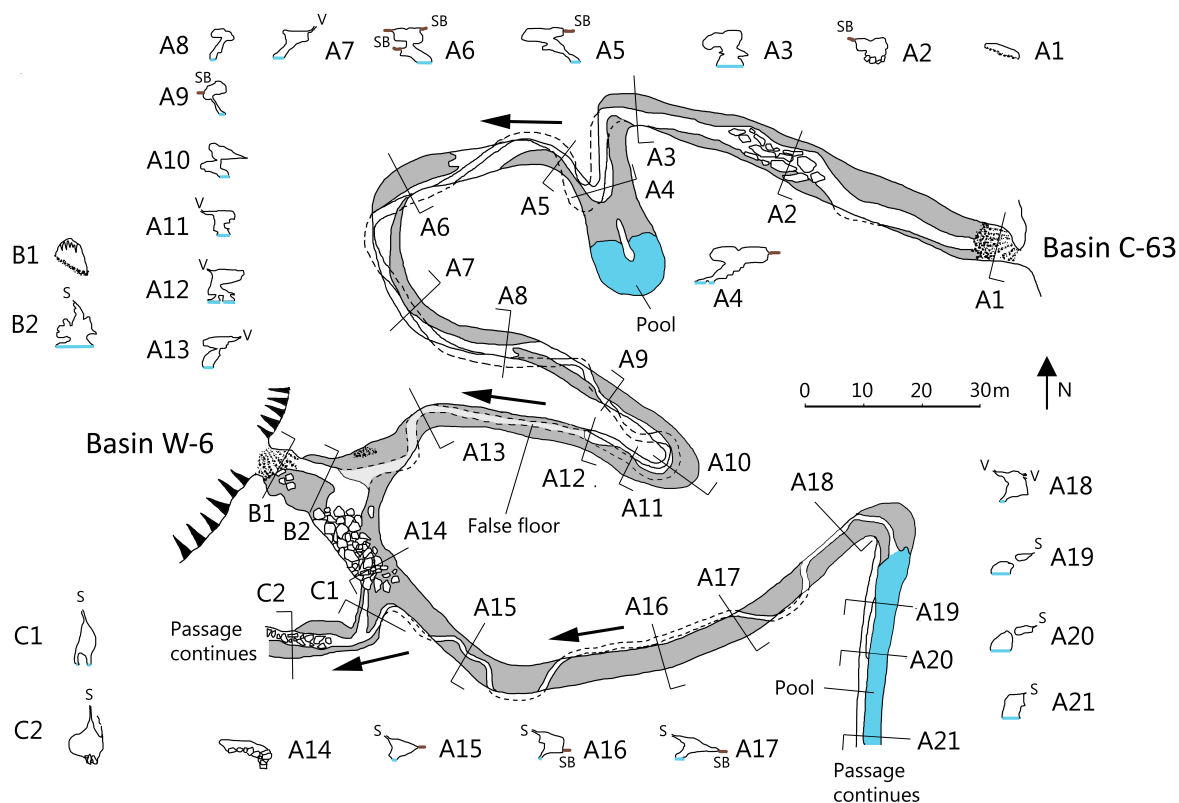


Fig. 3: Examples of surface topography, supraglacial meltwater channels and englacial conduit locations on Ngozumpa Glacier: a) DEM of the lower ablation zone of the glacier, based on GeoEye-1 stereo imagery from June 2010, showing location of enlarged panels and englacial conduit NG-05; b) supraglacial channels shown on the 2010 imagery; c) the same area shown on the 2010 DEM; d) hummocky debris-covered ice showing the boundaries of closed surface basins and locations of englacial conduits NG-01 to NG-03. Considerable basin expansion occurred in the 4 ablation seasons between the conduit surveys (December 2005) and the date of the DEM (June 2010); e) hummocky debris-covered ice and location of englacial conduit NG-04 (surveyed November 2009, 7 months before the date of the DEM). The dashed line in panel (a) shows the location of the long profile in Fig. 2.

918  
919  
920



921  
922 Fig. 4: Plan and passage cross sections of englacial conduit NG-04. SB: sediment band, S:  
923 suture, V: voids. Dark grey-filled and white-filled areas within the cave plan indicate the  
924 floors of the upper and lower levels, respectively. Pale grey and dashed lines are used where  
925 the lower level is occluded by higher false floors. Standing water on the cave floor is shown  
926 in blue. For location, see Fig. 3e.  
927

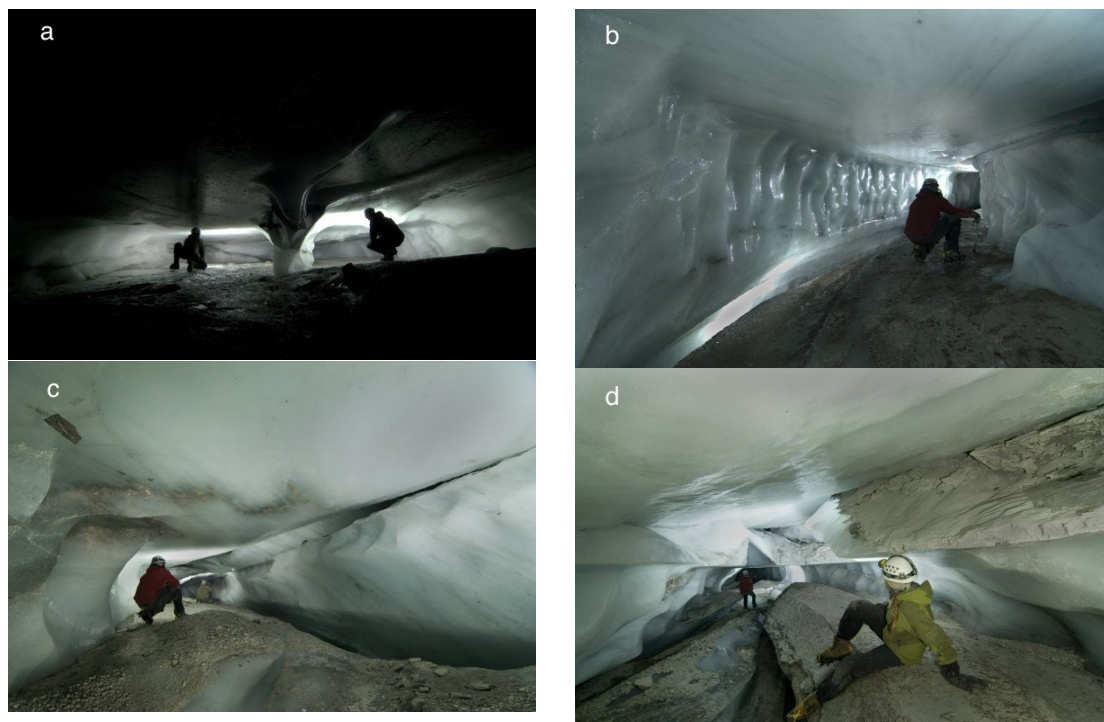




Fig. 5: Passage morphology in NG-04. a) Cutoff meander loop. Note inclined debris band on back wall behind the the left-hand figure. b) The upper passage near A12, showing suture between the right-hand wall and the ceiling, and the incised lower passage on the left. c) The upper passage near A7, with a void and suture between the right-hand wall and the ceiling. d) The upper passage near A6, showing a band of bedded sand filling a sub-horizontal suture above the foreground figure.

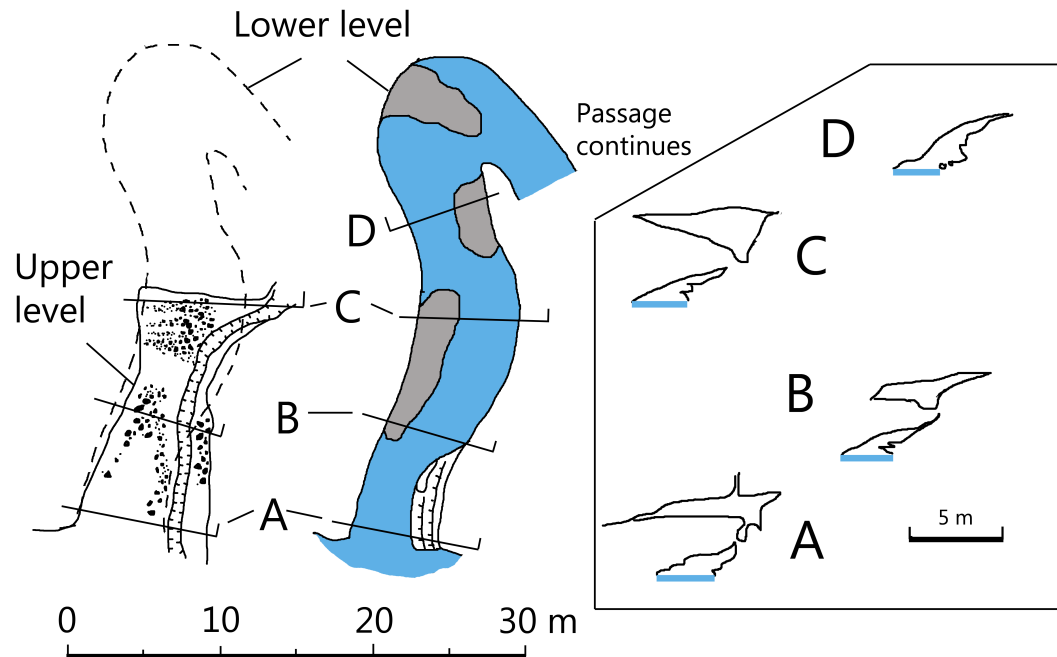


Fig. 6: Plan and passage cross sections of conduit NG-05. The plan view of the upper level shows boulders and an incised channel on the conduit floor. For location see Figure 3a.



Fig. 7: a) The entrance of NG-05 on the NW margin of Spillway Lake; b) NG-01: debris-filled canyon suture at the upper level of the cave; c) NG-01: flat-floored mid level of the cave. Note canyon suture above and incised lower level crossing foreground from left to right; d) NG-02: Tubular upper passage with canyon suture in the roof.

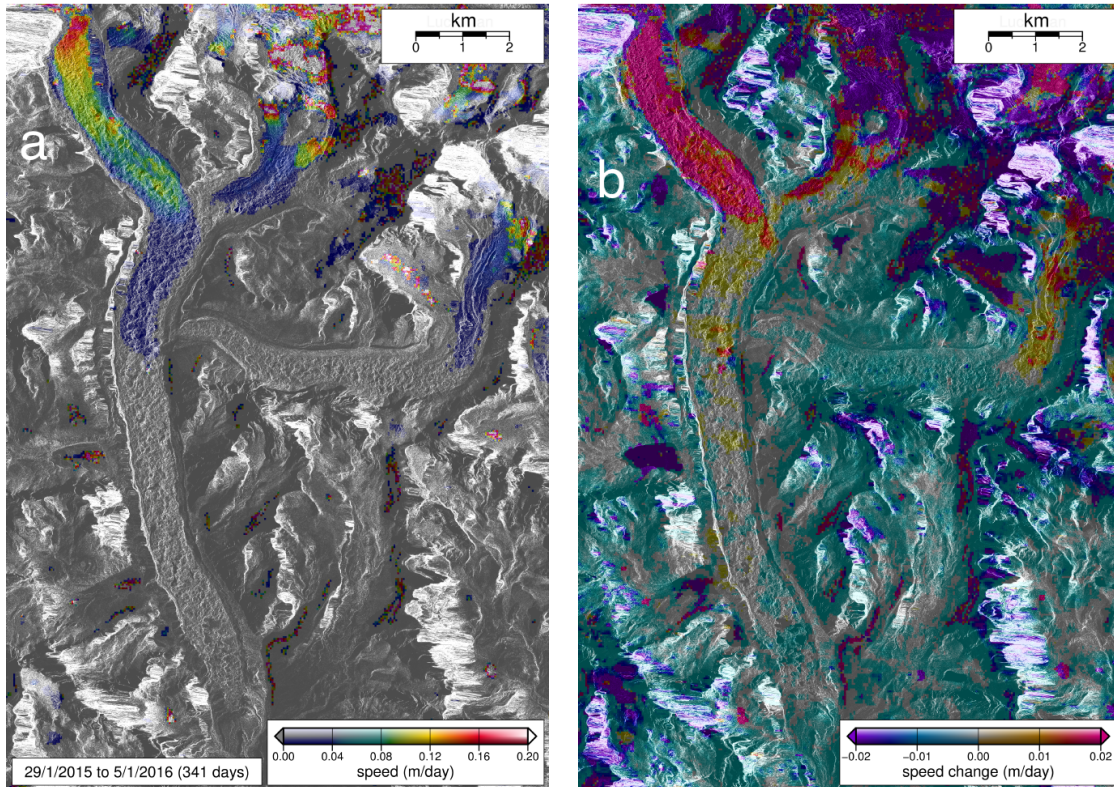


Fig. 8: Surface velocities derived from TerraSAR-X data: a) mean daily velocity for the 'annual' period (29 Jan 2015 to 5 Jan 2016); b) velocity difference between 'annual' period (29 Jan 2015 to 5 Jan 2016) and 'winter' period (19 Sept 2014 to 18 Jan 2015), indicating minimum summer speed-up of the glacier. No masks or filters were applied to the data.

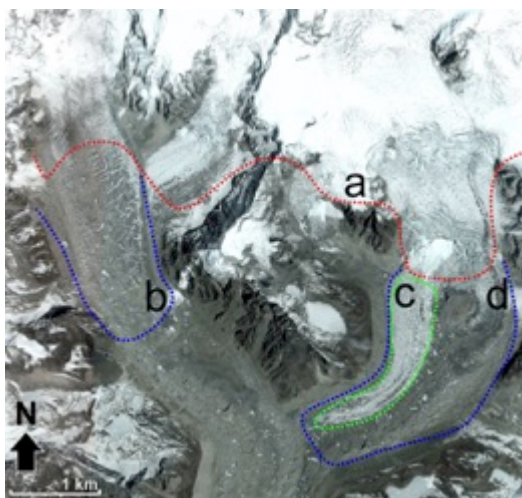


Fig. 9: Distribution of crevasses on the W and NE branches of Ngozumpa Glacier. (a) lower boundary of crevasse fields; (b, c, d) areas where supraglacial channels occur on debris-covered and clean (c) ice. Image source: Google Earth.



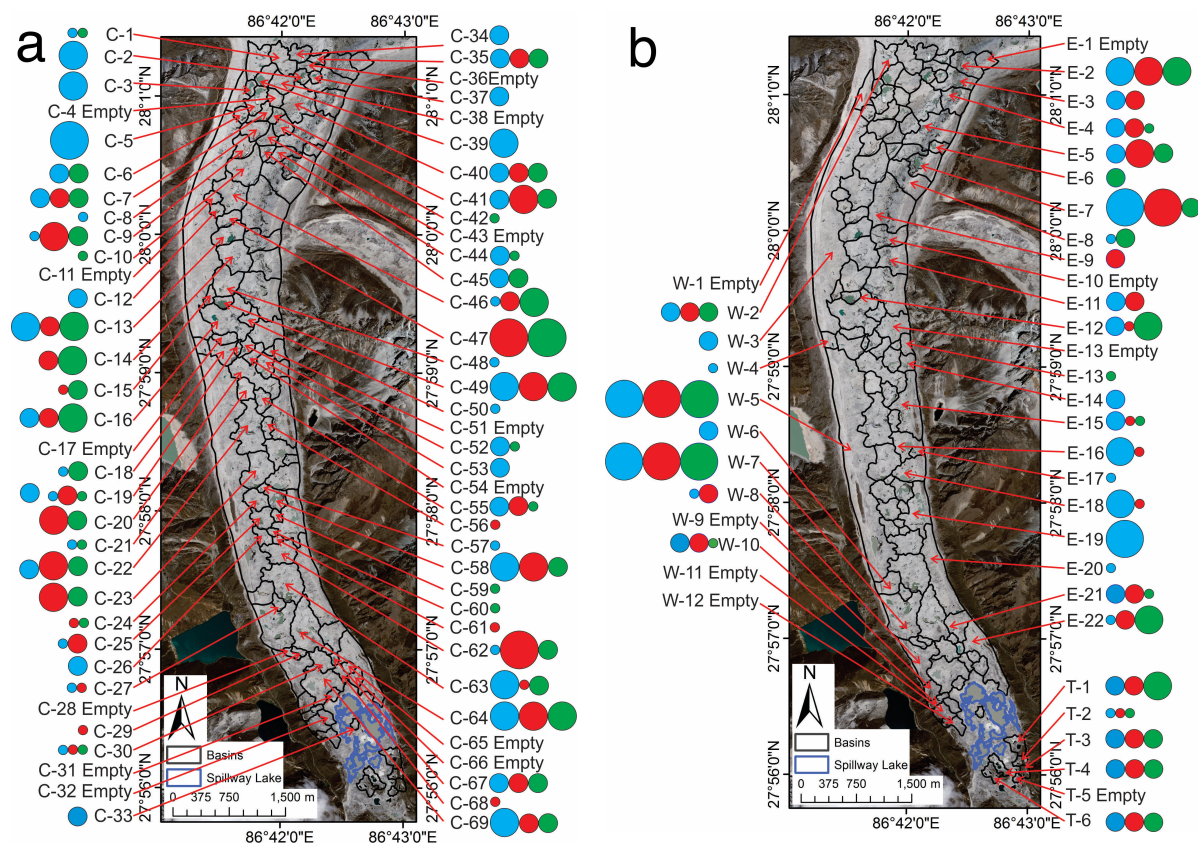


Fig. 10: Surface drainage basins and lake area changes: a) the central part of the glacier, and b) the lateral margins and terminal zone. Lake areas are shown for 2010 (blue), 2012 (red) and 2015 (green), in four categories: <1000 m<sup>2</sup> (small circles), 1000-5000 m<sup>2</sup> (medium circles), 5000-10000 m<sup>2</sup> (large circles) and >10000 m<sup>2</sup> (largest circles). Missing coloured circles indicate empty basins in that year.

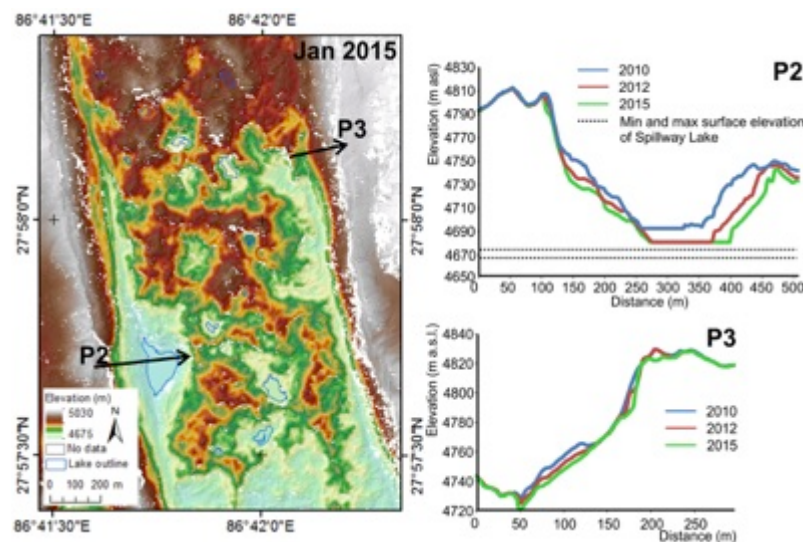


Fig. 11: Extract from the 2015 DEM and selected cross profiles in 2010, 2012 and 2015 showing lateral troughs, subsidence of trough floors and erosion of moraine slopes.

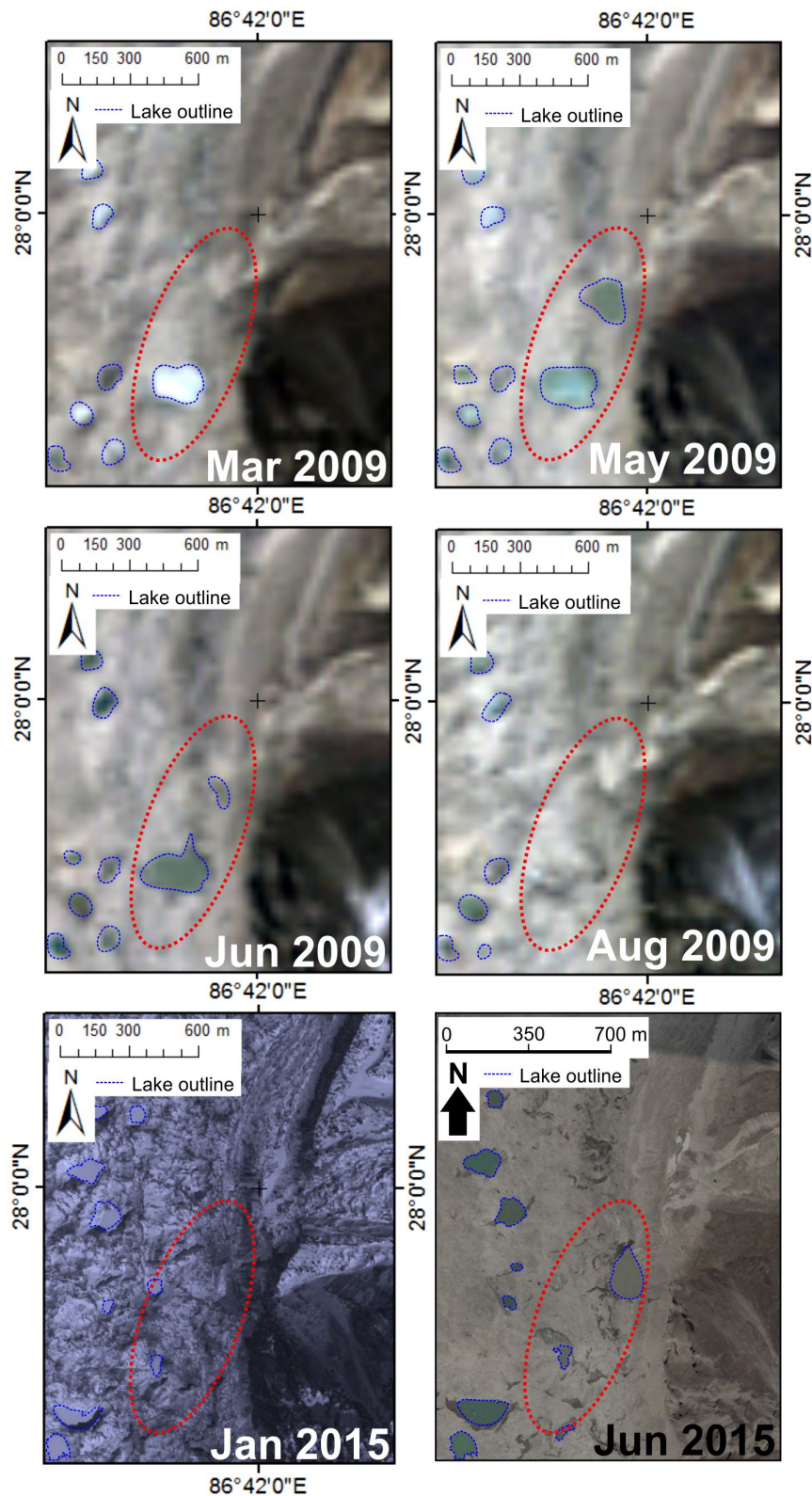


Fig. 12: Changing pond extent in Basin E-11, showing evidence of filling and drainage cycles. Pond outlines highlighted in blue.



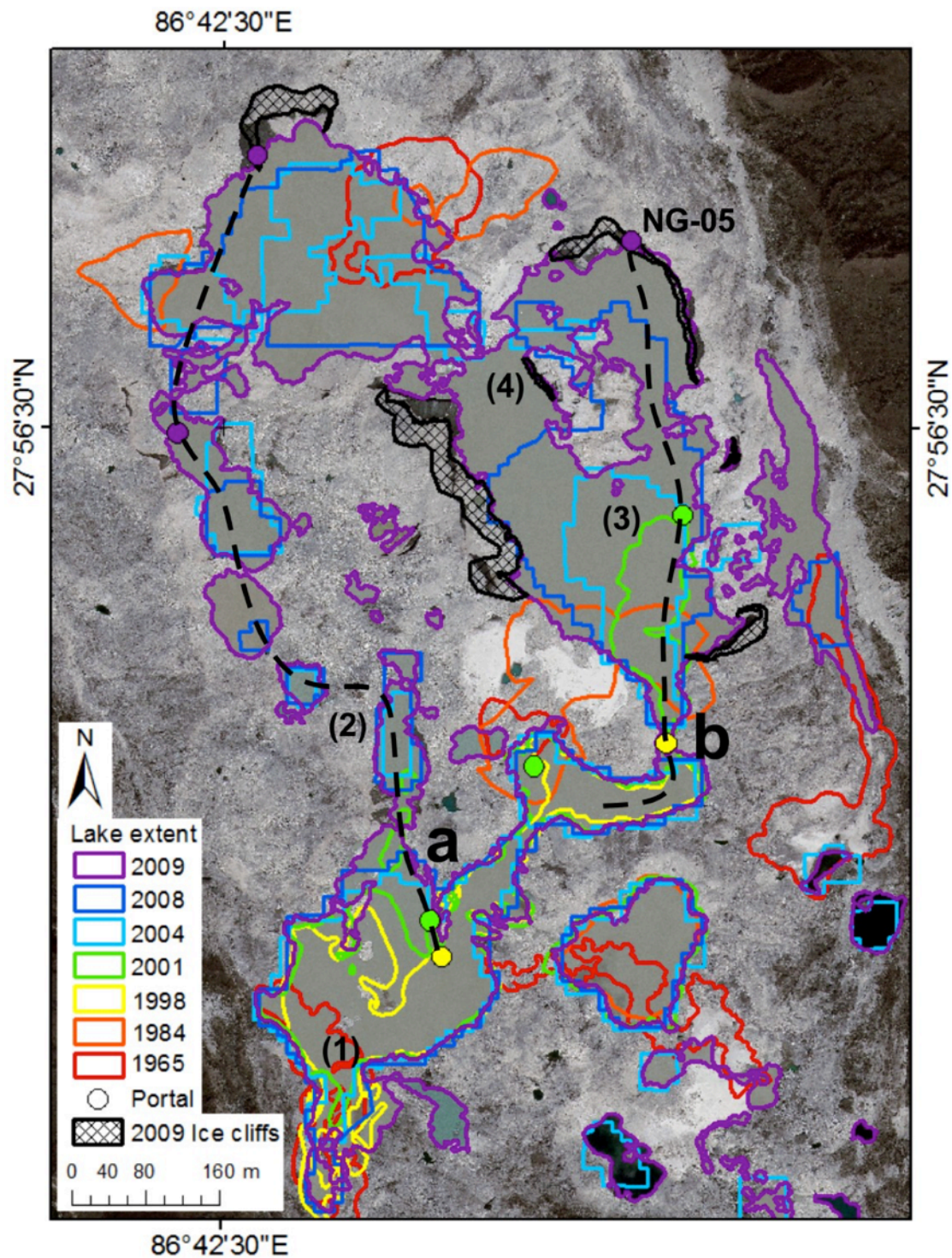


Fig. 13: Spillway Lake, 1965-2009, showing the position of meltwater portals and upwellings and the inferred location of englacial conduits (dashed lines). Background image: GeoEye-1 from June 2010. See text for explanation of lake evolution.



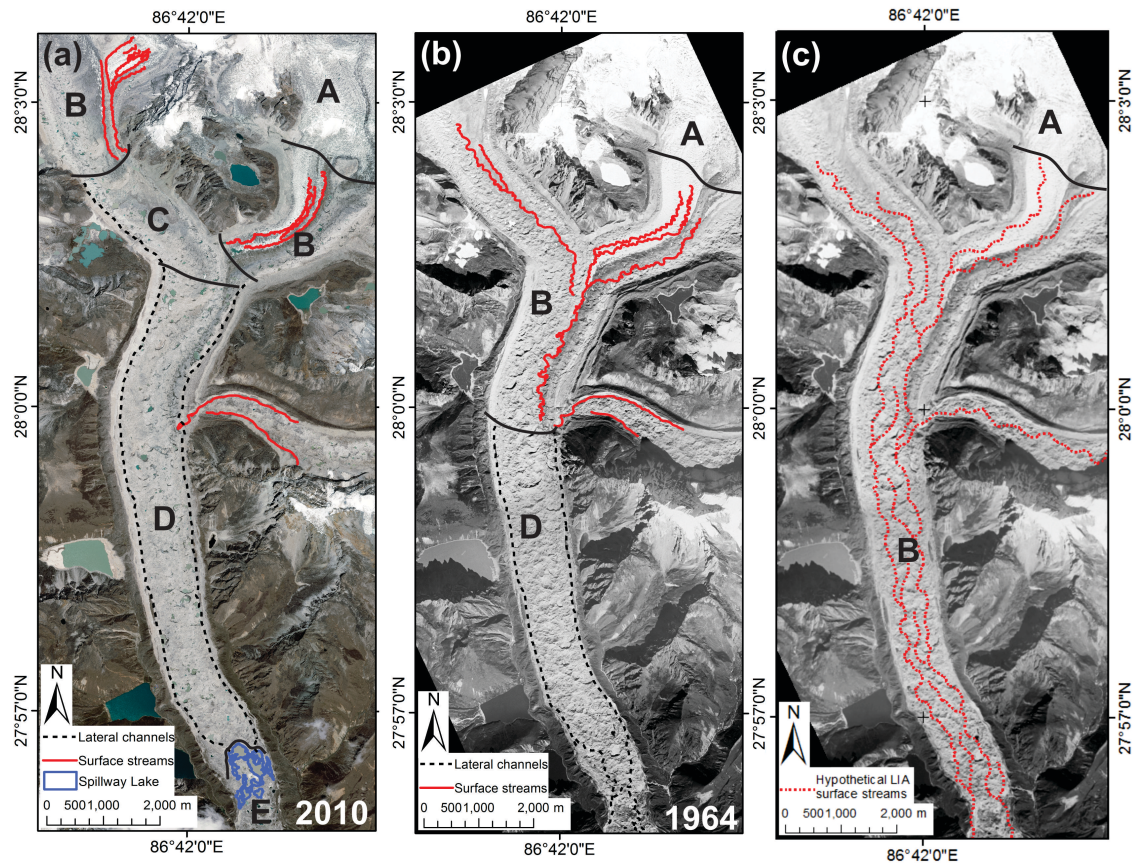


Fig. 14: Zonation of the drainage system in (a) 2010 (b) 1964 and (c) a hypothetical configuration at the Little Ice Age maximum. A: crevasse fields; B: supraglacial channels; C: transitional zone with shallow basins; D: closed surface basins with perched lakes; E: Spillway lake. Dashed black lines indicate the positions of sub-marginal conduits.

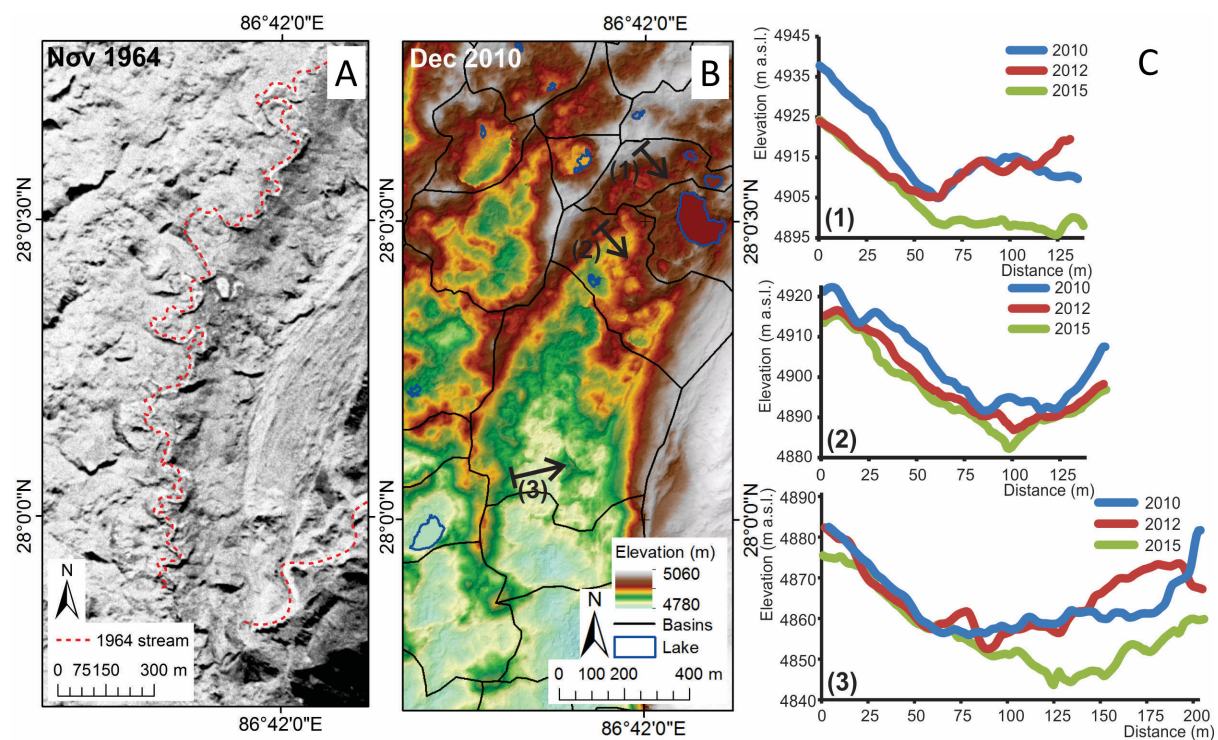


Fig. 15: Evolution of the eastern margin of the main trunk of Ngozumpa Glacier, 1964-2015. A: Supraglacial streams on the glacier surface in 1964 Corona imagery; B: 2010 DEM showing surface basins and the location of profiles; C: Surface profiles in 2010, 2012 and 2015, showing patterns of downwasting.

989 Table 1: Satellite imagery used in the paper

<b>Sensor</b>	<b>Product type</b>	<b>Resolution m</b>	<b>Acquisition date</b>	<b>Cloud cover (%)</b>
<b>Corona</b>	KH-4	3	04 Mar. 1965	-
<b>Landsat 5 TM</b>	Level T1	30	05 Mar. 2009	17
<b>Landsat 5 TM</b>	Level T1	30	08 May 2009	16
<b>Landsat 5 TM</b>	Level T1	30	09 Jun. 2009	28
<b>Landsat 5 TM</b>	Level T1	30	16 Aug. 2009	18
<b>GeoEye-1</b>	GeoStereo	PAN 0.46	09 Jun. 2010	3
	PAN/MSI	MSI 1.84		
<b>GeoEye-1</b>	GeoStereo	PAN 0.46	23 Dec. 2012	0
	PAN/MSI	MSI 1.84		
<b>WorldView-3</b>	GeoStereo	PAN 0.46	05 Jan. 2015	0
	PAN/MSI	MSI 1.84		

990